ACS APPLIED MATERIALS & INTERFACES

Research Article

Cite This: ACS Appl. Mater. Interfaces 2018, 10, 18281−18288

www.acsami.org

Novel Organic Phototransistor-Based Nonvolatile Memory Integrated with UV-Sensing/Green-Emissive Aggregation Enhanced Emission (AEE)-Active Aromatic Polyamide Electret Layer

Shun-Wen Cheng,[†,Δ] Ting Han,[‡,Δ] Teng-Yung Huang,[†] Yu-Hsin Chang Chien,[§] Cheng-Liang Liu,[*,§] Ben Zhong Tang,[*,‡] and Guey-Sheng Liou[*,†]

[†]Institute of Polymer Science and Engineering, National Taiwan University, Taipei 10617, Taiwan

[‡]Department of Chemical and Materials Engineering, Hong Kong University of Science and Technology, Clear Water Bay, Kowloon, Hong Kong, China

[§]Department of Chemical and Materials Engineering, National Central University, Taoyuan 32001, Taiwan

Supporting Information

ABSTRACT: A novel aggregation enhanced emission (AEE)-active polyamide **TPA-CN-TPE** with a high photoluminescence characteristic was successfully synthesized by the direct polymerization of 4-cyanotriphenyl diamine (**TPA-CN**) and tetraphenylethene (**TPE**)-containing dicarboxylic acid. The obtained luminescent polyamide plays a significant role as the polymer electret layer in organic field-effect transistors (OFETs)-type memory. The strong green emission of **TPA-CN-TPE** under ultraviolet (UV) irradiation can be directly absorbed by the pentacene channel, displaying a light-induced programming and voltage-driven erasing organic phototransistor-based nonvolatile memory. Memory window can be effectively manipulated between the programming and erasing states by applying UV light illumination and electrical field, respectively. The photoinduced memory behavior can be maintained for over 10^4 s between these two states with an on/off ratio of 10^4, and the memory switching can be steadily operated for many cycles. With high photoresponsivity (R) and photosensitivity (S), this organic phototransistor integrated with AEE-active polyamide electret layer could serve as an excellent candidate for UV photodetectors in optical applications. For comparison, an AEE-inactive aromatic polyimide **TPA-PIS** electret with much weaker solid-state emission was also applied in the same OFETs device architecture, but this device did not show any UV-sensitive and UV-induced memory characteristics, which further confirmed the significance of the light-emitting capability of the electret layer.

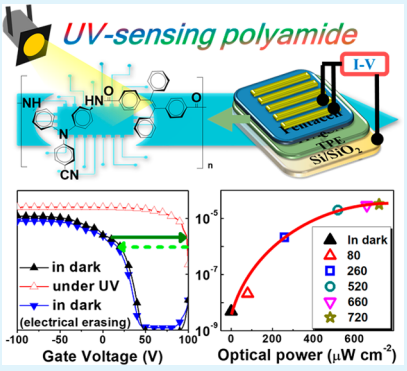

KEYWORDS: *organic phototransistor, nonvolatile memory, aggregation enhanced emission, photodetectors, polymer electret*

1. INTRODUCTION

Organic field-effect transistors (OFETs) have attracted tremendous attention from scientists. Compared with traditional inorganic materials-based transistors, organic materials enjoy the significant advantages of being lightweight and having low cost, flexibility, and a simple manufacturing process.[1−4] In particular, OFETs are superior to the widely used inorganic transistors in memory devices, because of their more-competitive manufacturing process than the traditional Si-based procedure. Using a polymeric memory is beneficial for practical applications, because of merits such as longer retention time, higher data storage density, and, most important of all, low power consumption. Devices of polymer memory could be classified into different categories according to the device structure and mechanism. Various types of OFET devices such as phototransistors, light-emitting transistors, light sensors, and transistor-type memory devices have been discussed.[5−8] Memory windows play an important role in OFET devices and great efforts have been devoted to enhancing memory windows, by synthesizing and introducing novel materials into OFET devices, optimizing available candidates, or designing novel device architectures.[9−14] Although many impressive accomplishments have been made, there are always limitations on the selection of suitable materials and architectures of devices. Consequently, it is crucial and highly desirable to develop novel materials for solving the current issues.

Photoinduced memory devices are the combination of phototransistor and transistor-type memory device. In recent years, researchers have been interested in the development of light controllable transistor devices, in which the memory window of devices can be manipulated by adjusting the light intensity.[15−17] When the OFET-type optical memory devices are exposed to light illumination, a large amount of excitons can

Received: February 10, 2018
Accepted: May 7, 2018
Published: May 7, 2018

DOI: 10.1021/acsami.8b02560
ACS Appl. Mater. Interfaces 2018, 10, 18281−18288

be generated in the organic semiconducting layer, which then are divided into electrons and holes in the presence of applied gate electric field. Subsequently, these charge carriers could be trapped in the underlying charge-storage layers, resulting in bistable current states via light-assisted programing and erasing processes.[18−21] In addition, because the memory behavior could be tuned by the intensity of light illumination, photodetectors and photosensors with different photoresponsivity (R) and photosensitivity (S) could be achieved.[22−24] To further utilize these effects, an AEE-active interlayer film can be incorporated into an OFET-type optical memory between the semiconductor and dielectric layers. Such an interlayer can influence the charge transport in semiconducting channel by altering the dipole moment and/or capacitance of dielectric films.[25−27]

Previously, some photoactive memory devices have been fabricated by using organic−inorganic complex/hybrid materials, organic semiconductors, and organic small molecules as the light emitters in the system.[28−36] Photoresponsive polymers and polymer−nanoparticle composite films have also been employed as interlayers of OFET-type memories to enhance the contribution of charge storage or trapped charge carrier effects.[27,37−44] However, the above-mentioned materials have some disadvantages, in terms of chemical resistance and thermal stability. To achieve memory devices with enhanced performance and applicability, luminescent polymers, such as aromatic high-performance polymers, and without decay of emission intensity caused by charge transfer effect,[44,45] are potential candidates to be used for phototransistor devices. Herein, the dual functions of memory devices and photodetectors were combined together. A novel organic phototransistor-based memory device shown in Figure 1 was

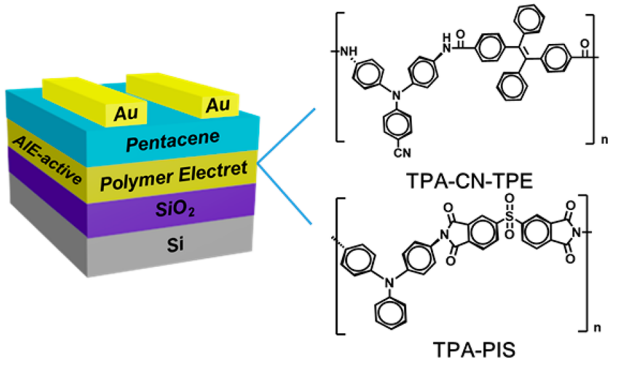

Figure 1. Organic phototransistor integrated with polymer electret layer of **TPA-CN-TPE** and **TPA-PIS**.

successfully prepared by using a single AEE-active aromatic polyamide **TPA-CN-TPE** as the electret layer. The photoluminecent (PL) polyamide emits strong green light under UV light irradiation. Such emission could be subsequently absorbed by the pentacene semiconducting channel. In this way, the memory window of the resulting transistor devices was significantly enhanced and can be manipulated between the light-induced programming state and the voltage-driven erasing state. By varying the intensity of the UV irradiation light source, an obvious shift of the threshold. voltage in the electrical transfer curves of OFETs was observed, indicating the characteristics of photodetector and photomemory could be successfully combined in one single device. The memory effect can maintain for at least 10^4 s even after removing the applied voltage. With high R and S value, this novel polymeric phototransistor-type memory device exhibits excellent UV sensing and memory properties while retaining good long-term stability and wide-range applicability. Meanwhile, the device based on weakly emissive aromatic polyimide **TPA-PIS** (without AEE moieties) was also prepared for comparison to further demonstrate the importance of light-emitting capability of the polymeric electret layer.

2. EXPERIMENTAL SECTION

2.1. Materials. 4,4′-Diamino-4′′-cyanotriphenylamine, 4,4′-diaminotriphenylamine, and 4,4′-(1,2-diphenylethene-1,2-diyl)dibenzoic acid were prepared according to previous literature.[46−51] All other solvents and reagents were used as received from commercial sources.

2.2. Device Fabrication and Measurements. Classic transistor-type memory devices were fabricated with the configuration of a top-contact device, which consists of a thermally grown 300-nm-thick SiO_2 dielectric on a highly doped n-type Si wafer. The wafer was cleaned by Piranha solution, which is composed of concentrated sulfuric acid and hydrogen peroxide. DMAc solutions of **TPA-CN-TPE** and **TPA-PIS** were filtered with a PTFE membrane syringe filter (pore size, 0.45 μm) and spin-coated with the condition of 60 s for 3000 rpm on a precleaned wafer. Then, the substrate heated at 150 °C for 30 min under nitrogen atmosphere to obtain polymer electret film with a thickness of ∼50 nm. Semiconducting pentacene thin films (50 nm) were thermally evaporated and deposited on the polymers at 10^{-7} Torr at 90 °C. Gold was then thermally evaporated on semiconductor layer as the source and drain for 50 nm with the shadow mask at the rate of 0.5 Å s^{-1}. The channel length of the device is 50 nm and the width is 1000 nm. The light source is 365 nm UV light, and the UV intensity is measured by a photometer. The properties of OFET devices were measured by a Keithley 4200-SCS device at room temperature under inert condition. The PL intensity in the solid state was determined using a calibrated integrating sphere, and the absorbance of the measuring sample was controlled in the range of 0.1−0.15 by adjusting the thickness of the polymer film.

3. RESULTS AND DISCUSSION

3.1. Polymer Synthesis and Characterization. As shown in Scheme S1a in the Supporting Information, an AEE-active polyamide **TPA-CN-TPE** was synthesized from the direct polymerization of 4-cyanotriphenyl diamine (**TPA-CN**) and tetraphenylethene (**TPE**)-containing dicarboxylic acid. An aromatic polyimide (**TPA-PIS**) was also prepared by the polymerization route shown in Scheme S1b in the Supporting Information. The detailed synthetic procedure can be found in the Supporting Information. The chemical structure of **TPA-CN-TPE** was confirmed by FT-IR and NMR spectra, as depicted in Figures S1 and S2 in the Supporting Information. The obtained polyamide can be readily dissolved in aprotic organic solvents, such as dimethylsulfoxide (DMSO), dimethylacetamide (DMAc), dimethylformamide (DMF), and N-methyl-2-pyrrolidone (NMP) solvents, and can be easily fabricated into transparent films by solution-casting. The TGA and DSC traces of **TPA-CN-TPE** are provided in the Figures S3 and S4 in the Supporting Information. All the thermal properties, inherent viscosity, the molecular weight and solubility behavior of the synthesized **TPA-CN-TPE** are summarized in Tables S1−S3 in the Supporting Information.

3.2. Photophsyical Properties of the Polymer Electret and Pentacene Films. The polymer **TPA-CN-TPE** shows an aggregation-enhanced emission (AEE) effect. When water is added into a NMP solution of the **TPA-CN-TPE**, nanoaggregates of the polymer are formed and its PL is enhanced. The PL intensity is gradually increased with increasing water

DOI: 10.1021/acsami.8b02560
ACS Appl. Mater. Interfaces 2018, 10, 18281−18288

fraction (f_w) in the NMP−water mixture (Figures S5 and S6 in the Supporting Information). To discuss the interlayer optical interaction between the polymers (**TPA-CN-TPE** and **TPA-PIS**) and the pentacene semiconductor, the UV-vis absorption and photoluminescence (PL) spectra of their spin-coated films on quartz glasses were first investigated. The UV-vis absorption spectra of **TPA-CN-TPE**, **TPA-PIS**, and deposited pristine pentacene films are compared in Figure 2a, and the PL spectra

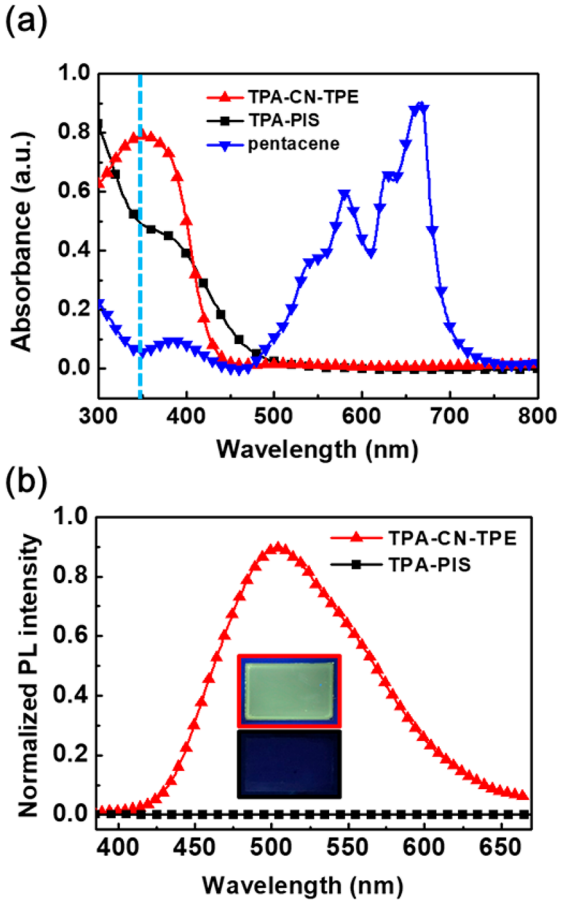

Figure 2. (a) UV−vis absorption spectra of the films of **TPA-CN-TPE**, **TPA-PIS**, and pentacene. The blue vertical dash line denotes the location of 365 nm wavelength. (b) PL spectra of the **TPA-CN-TPE** and **TPA-PIS** films and the associated photos taken under UV irradiation. Excitation wavelength = 365 nm.

of **TPA-CN-TPE** and **TPA-PIS** are depicted in Figure 2b. The maximum absorbance and PL intensity for **TPA-CN-TPE** film is located at wavelengths of 343 and 510 nm, respectively. Thus, the polyamide film can show strong green emission when excited with UV light ranging from 325 to 400 nm. The absorption spectrum of pentacene in Figure 2a indicated that the emission of **TPA-CN-TPE** could be further absorbed by the pentacene semiconductor film. On the other hand, aromatic polyimide **TPA-PIS** film only exhibited very weak luminescence, because of the existence of a much stronger intramolecular charge transfer effect than that of **TPA-CN-TPE**. The PL spectra of pristine **TPA-CN-TPE** film and **TPA-CN-TPE**/pentacene bilayer film were obtained in Figure S7 in the Supporting Information when excited at 343 nm. Both films exhibited the emission peak at ∼500 nm. In contrast to the pristine **TPA-CN-TPE** film, the **TPA-CN-TPE**/pentacene bilayer film shows a decrease in PL intensity, indicating that the top pentacene may induce more effective excitons to be dissociated between the **TPA-CN-TPE**/pentacene interface.

3.3. Electrical Characteristics of the Charge-Trapping Memory Devices. The bottom-gate top-contact (BGTC) OFETs containing one additional **TPA-CN-TPE** or **TPA-PIS** polymer electret layers were prepared (Figure 1). A large shift in threshold voltage (V_{th}) in the transfer curve of **TPA-CN-TPE** polyamide electret containing organic phototransistor was observed under 720 μW cm^{-2} UV illumination (Figure 3). The

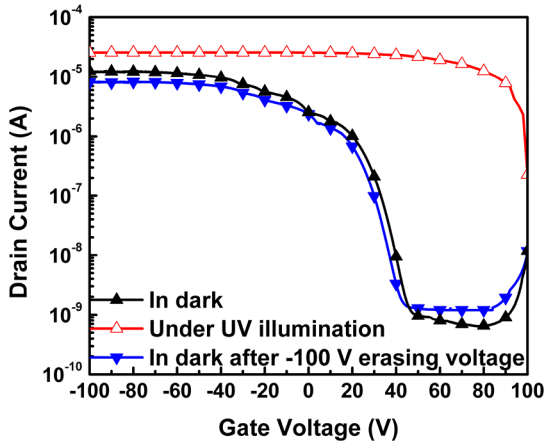

Figure 3. Transfer curves of the organic phototransistor with **TPA-CN-TPE** electret measured in darkness, under UV illumination with the intensity of 720 μW cm^{-2} for 1 s, and then in darkness after electrical erasing with applied gate voltage (V_g) of −100 V for 1 s.

drain current (I_d) increased significantly by UV excitation without any applied voltage bias, because the photoinduced charge carriers could be generated in the pentacene layer under UV irradiation and charges could be trapped in the electret layer as an electric field is applied. After treating the OFET with −100 V, the transfer curve shifted negatively back to the original state, denoting a voltage-driven erasing process. In order to more deeply confirm how the assistance of photoenhanced charges affects the memory behavior, the electrical measurements with and without 720 μW cm^{-2} UV illumination were operated for **TPA-CN-TPE** and **TPA-PIS** electret-containing OFETs, respectively (see Figure 4). The programming and erasing process were operated with applied gate voltage (V_g) values of 100 and −100 V, respectively, for 15 s. The UV illuminating time was 1 s for each measurement. For **TPA-CN-TPE** electret-based OFETs, an obvious increase in the memory window, increased from 20 V to 42 V, can be observed after the assistance of UV light illumination, which was indicated by the blue dash lines in Figure 4a. This result indicated that the additional charges can be effectively induced by UV illumination. Since the OFETs based on **TPA-PIS** electret could not show comparable PL property, the charges in semiconducting layer of the phototransistor are difficult to be further induced by UV illumination. As a result, **TPA-PIS** electret-based OFETs with weak PL property exhibited almost no change in the memory window (Figure 4b).

Adjustable shifts in the V_{th} of the organic phototransistors could be used to achieve the multilevel charge storage. We performed this specific photomemory effect by modulating the UV light power from 720 to 80 μW cm^{-2} without any applied bias. Different shifts of the V_{th} in transfer curves could be obtained obviously by varying the intensities of UV illumination

DOI: 10.1021/acsami.8b02560
ACS Appl. Mater. Interfaces 2018, 10, 18281−18288

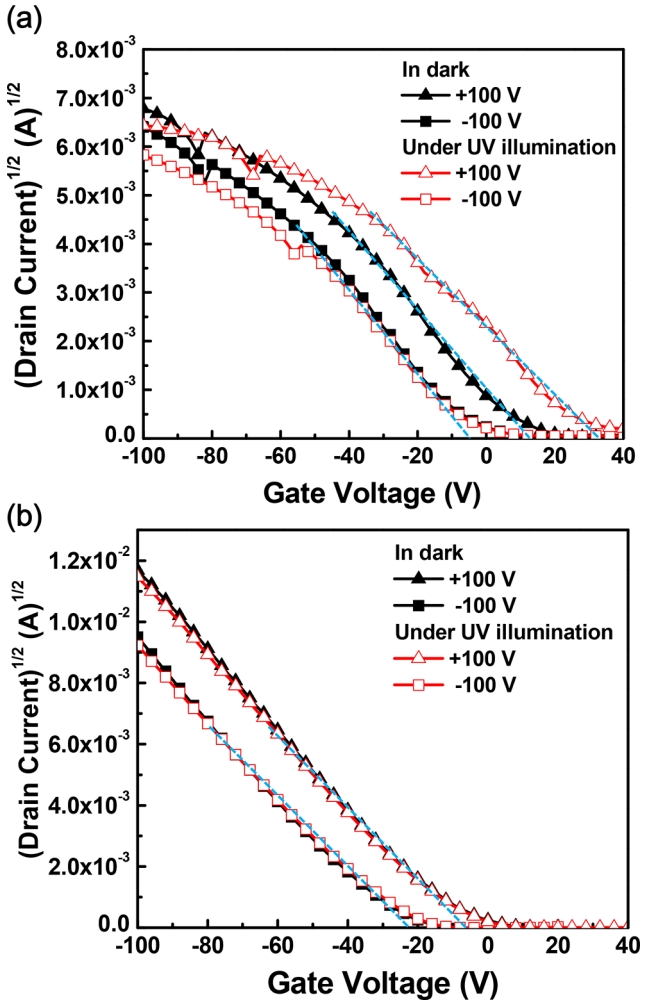

Figure 4. Transfer curves of the organic phototransistors based on (a) **TPA-CN-TPE** and (b) **TPA-PIS** electret layers, respectively, with/without 720 μW cm^{-2} UV illumination for 1 s and after 100 V or −100 V were operated. The memory window is defined from the V_{th} difference between two blue dotted lines in the diagram. The programming and erasing V_g values are 100 V and −100 V, respectively, applied for 15 s.

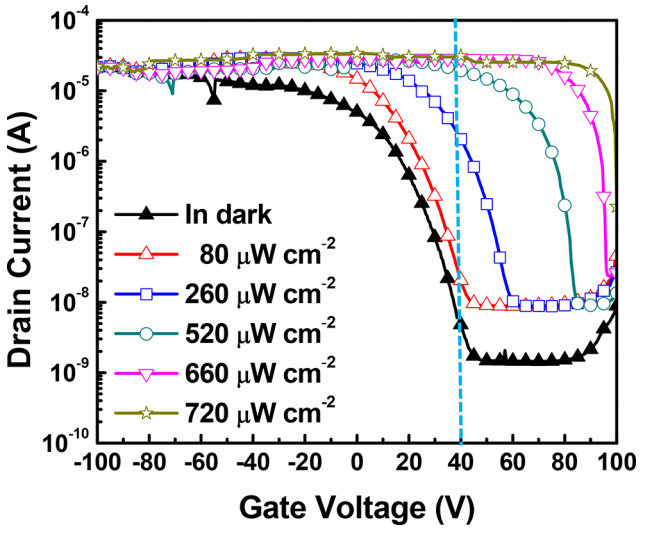

Figure 5. Shift of transfer curves for the organic phototransistor based on the **TPA-CN-TP** electret under different intensity of incident UV irradiation.

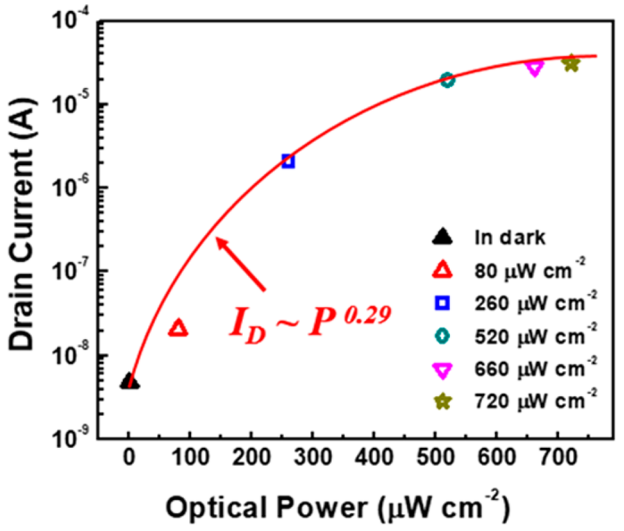

Figure 6. I_d curve fitting (at V_g = 40 V) of the organic phototransistor based on **TPA-CN-TP** electret at various UV intensities.

with a fixed time of 1 s for each measurement (see Figure 5). Note that a −100 V bias was applied to reset the memory device back to the initial state between each transfer curve scans. The results reveal a positively shifted V_{th} and an enhanced I_d with increasing UV light intensity. Therefore, different memory states can be achieved if the reading voltage was applied (for example, 40 V in this case), representing the multilevel charge storage. Based on the transfer curves measured under various UV light intensities (Figure 5), I_d photoresponse at V_g = 40 V could be plotted as a function of the UV light intensity (see Figure 6, where the organic phototransistors obtained the most significant sensing effect). The photocurrent amplitude was strongly dependent on the light power, and the dependence obeys a power law of eq 1,[52−55]

$$I_d = cP^k \quad (1)$$

where P is the light intensity, c a proportionality constant, and k an empirical value. By fitting the experimental data with eq 1, values of c = 13 372 and k = 0.29 could be obtained. This relationship further demonstrated that the photocurrent was exactly from the contribution of accumulated photo-excited charge in the electret layer. The minimum sensible optical power was 80 μW cm^{-2}, which could be used to calculate the dynamic range (DR) value, which Tong and Forrest have shown an optical sensor based on subphthalocyanine (SubPc) with a DR value of 12 bits for monochromic light with a wavelength of 580 nm. The DR value of photoelectric sensor is defined as eq 2,

$$\mathrm{DR} = \log_2\left(\frac{I_{ill,max} - I_{dark}}{I_{ill,min} - I_{dark}}\right) \quad (2)$$

where $I_{ill,max}$ and $I_{ill,min}$ are the maximum and minimum sensible current change under the programming bias and UV illumination, respectively. If the intensity of UV illumination was lower than 80 μW cm^{-2}, the photoresponse of organic phototransistor was insensitive to the light. Afterward, a rapid increase in the I_d can be observed with an increase in UV

DOI: 10.1021/acsami.8b02560
ACS Appl. Mater. Interfaces 2018, 10, 18281−18288

intensity, because of the photogenerated charge carriers from the absorbed flux. On the other extreme, the output current response reached the saturated state when the intensity of UV illumination was larger than 720 μW cm^{-2}, possibly because the recombination and generation of charge carriers were balanced under the UV irradiation. Based on eq 1 and the I_{dark} = 4.78 × 10^{-9} A obtained from the transfer curve in Figure 5, the DR value for this organic phototransistor was determined to be 14 bits, suggesting a high performance organic photodetector. This significant improvement of the DR value could be attributed to the low off current and the large shift in V_{th}, measuring from the transfer curves under UV illumination for 1 s in each measurement (programming process). The other two important parameters for a quantifying organic phototransistor, i.e., photoresponsivity (R) and photosensitivity (S), can be estimated by eqs 3 and 4,[56]

$$R = \frac{I_{ill} - I_{dark}}{P_{ill}} \quad (3)$$

$$S = \frac{I_{ill} - I_{dark}}{I_{dark}} \quad (4)$$

where $I_{ill} - I_{dark}$ is the difference between I_d under UV illumination and in darkness, and P_{ill} is the incident optical power on the channel.

The dependence of R and S on UV light intensity (at V_g = 40 V) is depicted in Figure 7. The R value indicates how much

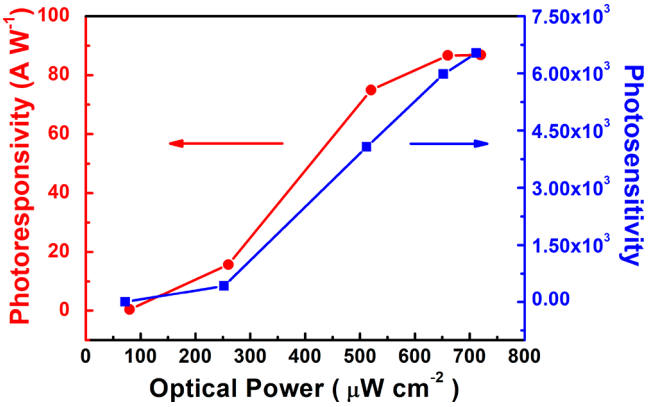

Figure 7. R and S values of the organic phototransistor based on **TPA-CN-TP** electret under different intensity of incident UV irradiation for 1 s (at V_g = 40 V).

light is absorbed, compared to how much light reaches the device. The parameter S has many parallels to a signal-to-noise ratio. R and S gradually increase as the UV light intensity increasing from 80 to 720 μW cm^{-2}, which could be attributed to the existence of the charge trapping. Thus, the enhanced photoexcited I_d value determined by the amount of photoinduced charge carriers under light illumination could be explained by this phenomenon. The maximum R value is 90 A W^{-1} at P_{ill} of 720 μW cm^{-2}, while the maximum S value is 6500. Compared with the conventional phototransistor or photodiode, the increase of device current is directly related to the generation of the photoexcited carriers in the active channel from the light input, providing a direct response to the light input. However, for the organic phototransistor fabricated in this work, AEE-active polymer with wide energy band gap as electret layer was intentionally introduced to trap charges by the programming voltage bias. Thus, more charges being trapped can be further controlled by tuning the incident UV light intensity at a particular programming bias. The mobile electrons generated by excitons in pentacene channel under the green light emission of **TPA-CN-TPE** layer would be possibly trapped by the **TPA-CN-TPE** electret if a positive V_g is applied to the device. The accumulation of trapped electrons is beneficial for the channel formation of OFETs at a lower V_g, resulting in a positive shift of V_{th} of the OFETs. Subsequently, I_d increases even at a low V_g, indicating that the obtained device by this approach manifest the dual functions of memory and photosensing characteristics. Furthermore, a negative V_g that is used in an erasing process can further reset the device to the initial state and make it ready for reprogramming in the next round of the entire memory operation.

The capability of high current retention over long time implies that the device with the AEE-active **TPA-CN-TPE** electret could function not only as a photodetector but also a light-induced memory device, and the resulting organic phototransistor can maintain stable charging states after the programming and erasing processes (Figure 8). The red and

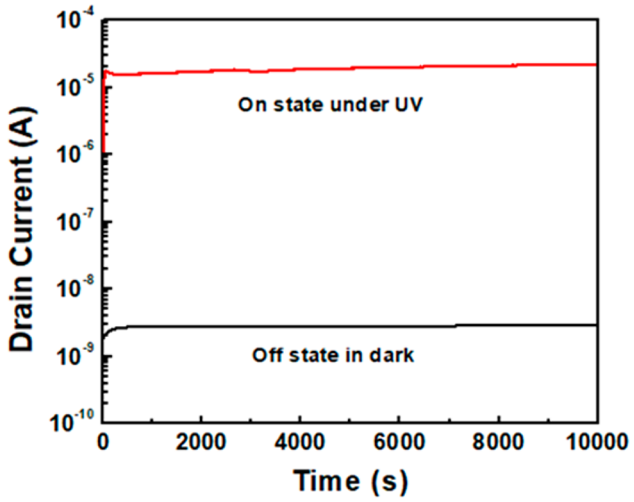

Figure 8. Retention time test of the organic phototransistor based on **TPA-CN-TP** electret: the "on" state (red line) was measured under an UV intensity of 720 μW cm^{-2} for 1 s with a V_g reading of 40 V; the "off" state (the black line) was measured in darkness, using a value of V_g = 40 V.

black lines of high (1 × 10^{-5} A) and low (2 × 10^{-9} A) I_d values represent the "on" and "off" states of the organic phototransistor-type memory device (high current contrast on/off ratio of 10^4) measured at V_g of 40 V, respectively, where the photoinduced I_d of the device allows for ∼10^4 s after the UV irradiation source was removed.

The multiple switching stability of the organic phototransistor-type memory device with **TPA-CN-TPE** polyamide electret was measured at V_g = 40 V and V_d = −100 V. The results are depicted in Figure 9, where the device was periodically irradiated under UV illumination at 365 nm for 1 s and with an erasing V_g of −100 V. Careful analysis of the data reveals that each measuring cycle provides a UV response plot. The device responds fast enough to afford a sharp jump of photoinduced I_d (∼10^4 on/off current ratio) under the green emission from the **TPA-CN-TPE** electret. By applying a pulse of V_g of −100 V, which was found to be a strong enough

DOI: 10.1021/acsami.8b02560
ACS Appl. Mater. Interfaces 2018, 10, 18281−18288

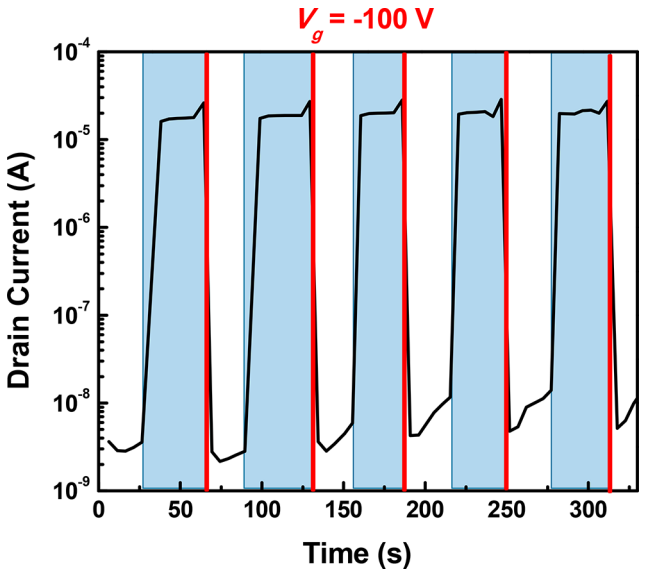

Figure 9. Real-time I_d response upon dynamic on/off switching. The reading voltage bias was fixed at 40 V. The intensity of UV illumination is 720 μW cm^{-2}. (The white space represents readings in darkness; the blue space represents readings after 1 s of UV illumination).

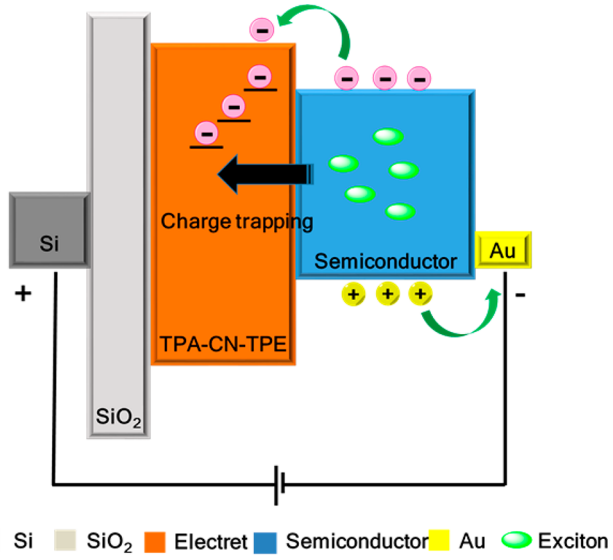

Figure 10. Operation mechanism for the organic phototransistor memory device based on **TPA-CN-TPE** polyamide electret.

negative voltage to immediately return the memory device back the low current state (off state), the subsequent specific UV irradiation to recover the high current on-state for reprogramming, and the dynamic on/off switching can be operated consistently. Based on the above-mentioned results, the significantly fast UV response capability and the ability to reset the device, together with the long-term retention time, allow the presented organic phototransistor with an AEE-active **TPA-CN-TPE** polyamide electret to find promising applications in nonvolatile flash photomemory or as a photodetector.

3.4. Operation Mechanism. In our system, the AEE-active **TPA-CN-TPE** polyamide film absorbs the UV light first and then emits strong green light (~510 nm), which could be absorbed by the top pentacene layer to generate excitons (hole−electron pairs) in the pentacene (Figure 10). After treating the devices with electric bias, the photoinduced excitons would be separated. Consequently, the photocurrent could be formed after efficient charge separation and trapping of electron in the electret layer, resulting in a larger memory window, compared with the system in darkness.

4. CONCLUSION

A novel AEE-active **TPA-CN-TPE** polyamide was successfully synthesized and introduced as an electret layer in the organic phototransistor-type memory device. The strong green emission of **TPA-CN-TPE** under UV illumination can increase the memory window of the device ranging from 20 to 42 V, because of the photoinduced charges from the pentacene layer. The high R and S of the obtained devices manifest its great potential for multinary data storage and photodetector within a single device. With the significant photoinduced charge trapping in the **TPA-CN-TPE** electret layer, the device reveals a high DR of up to 14 bits. Therefore, this work offers a facile and efficient design concept for the fabrication of highly UV-responsive phototransistors for UV sensors and nonvolatile memory devices on data storage application.

■ ASSOCIATED CONTENT

Supporting Information

The Supporting Information is available free of charge on the ACS Publications website at DOI: 10.1021/acsami.8b02560.

Polymer synthesis, IR and NMR spectra, TGA and DSC traces, fluorescent spectra and photographs, and the summary of inherent viscosity and molecular weight of the polyamide **TPA-CN-TPE** (PDF)

■ AUTHOR INFORMATION

Corresponding Authors

*E-mail: clliu@ncu.edu.tw (C.-L. Liu).
*E-mail: tangbenz@ust.hk (B. Z. Tang).
*E-mail: gsliou@ntu.edu.tw (G.-S. Liou).

ORCID

Ting Han: 0000-0003-1521-6333
Cheng-Liang Liu: 0000-0002-8778-5386
Ben Zhong Tang: 0000-0002-0293-964X
Guey-Sheng Liou: 0000-0003-3725-3768

Author Contributions

[Δ]These authors contributed equally to this work.

Notes

The authors declare no competing financial interest.

■ ACKNOWLEDGMENTS

This work was financially supported by the Advanced Research Center of Green Materials Science and Technology from The Featured Area Research Center Program within the framework of the Higher Education Sprout Project by the Ministry of Education (107L9006) and the Ministry of Science and Technology in Taiwan (MOST 106-2218-E-002-021-MY2 & 107-3017-F-002-001).

■ REFERENCES

(1) Klauk, H. Organic Thin-film Transistors. *Chem. Soc. Rev.* **2010**, *39* (7), 2643−2666.
(2) Wen, Y.; Liu, Y.; Guo, Y.; Yu, G.; Hu, W. Experimental Techniques for the Fabrication and Characterization of Organic Thin

DOI: 10.1021/acsami.8b02560
ACS Appl. Mater. Interfaces 2018, 10, 18281−18288

Films for Field-Effect Transistors. *Chem. Rev.* **2011**, *111* (5), 3358−3406.
(3) Zilberberg, K.; Meyer, J.; Riedl, T. Solution Processed Metal-Oxides for Organic Electronic Devices. *J. Mater. Chem. C* **2013**, *1* (32), 4796−4815.
(4) Han, S. T.; Zhou, Y.; Roy, V. Towards the Development of Flexible Non-volatile Memories. *Adv. Mater.* **2013**, *25* (38), 5425−5449.
(5) Gwinner, M. C.; Kabra, D.; Roberts, M.; Brenner, T. J.; Wallikewitz, B. H.; McNeill, C. R.; Friend, R. H.; Sirringhaus, H. Highly Efficient Single-Layer Polymer Ambipolar Light-Emitting Field-Effect Transistors. *Adv. Mater.* **2012**, *24* (20), 2728−2734.
(6) Yu, H.; Bao, Z.; Oh, J. H. High-Performance Phototransistors Based on Single-Crystalline n-Channel Organic Nanowires and Photogenerated Charge-Carrier Behaviors. *Adv. Funct. Mater.* **2013**, *23* (5), 629−639.
(7) Wakayama, Y.; Hayakawa, R.; Seo, H.-S. Recent Progress in Photoactive Organic Field-effect Transistors. *Sci. Technol. Adv. Mater.* **2014**, *15* (5), 024202.
(8) Zhou, Y.; Han, S. T.; Sonar, P.; Roy, V. Nonvolatile Multilevel Data Storage Memory Device from Controlled Ambipolar Charge Trapping Mechanism. *Sci. Rep.* **2013**, *3*, 2319.
(9) Zhuang, J.; Han, S. T.; Zhou, Y.; Roy, V. Flash Memory Based on Solution Processed Hafnium Dioxide Charge Trapping Layer. *J. Mater. Chem. C* **2014**, *2* (21), 4233−4238.
(10) Hong, A. J.; Song, E. B.; Yu, H. S.; Allen, M. J.; Kim, J.; Fowler, J. D.; Wassei, J. K.; Park, Y.; Wang, Y.; Zou, J.; Kaner, R. B.; Weiller, B. H.; Wang, K. L. Graphene Flash Memory. *ACS Nano* **2011**, *5* (10), 7812−7817.
(11) Burkhardt, M.; Jedaa, A.; Novak, M.; Ebel, A.; Voïtchovsky, K.; Stellacci, F.; Hirsch, A.; Halik, M. Concept of a Molecular Charge Storage Dielectric Layer for Organic Thin-Film Memory Transistors. *Adv. Mater.* **2010**, *22* (23), 2525−2528.
(12) Chiu, Y. C.; Chen, T. Y.; Chen, Y.; Satoh, T.; Kakuchi, T.; Chen, W. C. High-Performance Nonvolatile Organic Transistor Memory Devices Using the Electrets of Semiconducting Blends. *ACS Appl. Mater. Interfaces* **2014**, *6* (15), 12780−12788.
(13) Pan, T. M.; Yeh, W. W. A High-k Y 2 O 3 Charge Trapping Layer for Nonvolatile Memory Application. *Appl. Phys. Lett.* **2008**, *92* (17), 173506.
(14) Baeg, K. J.; Noh, Y. Y.; Ghim, J.; Kang, S. J.; Lee, H.; Kim, D. Y. Organic Non-Volatile Memory Based on Pentacene Field-Effect Transistors Using a Polymeric Gate Electret. *Adv. Mater.* **2006**, *18* (23), 3179−3183.
(15) Gao, X.; Liu, C. H.; She, X. J.; Li, Q. L.; Liu, J.; Wang, S. D. Photon-Energy-Dependent Light Effects in Organic Nano-floating-gate Nonvolatile Memories. *Org. Electron.* **2014**, *15* (10), 2486−2491.
(16) Han, S. T.; Zhou, Y.; Yang, Q. D.; Lee, C. S.; Roy, V. A. L. Nanocomposite: Poly(3-hexylthiophene)/Gold Nanoparticle Hybrid System with an Enhanced Photoresponse for Light-Controlled Electronic Devices (Part. Part. Syst. Charact. 7/2013). *Particle & Particle Systems Characterization* **2013**, *30* (7), 646−646.
(17) Dutta, S.; Narayan, K. Gate-Voltage Control of Optically-Induced Charges and Memory Effects in Polymer Field-Effect Transistors. *Adv. Mater.* **2004**, *16* (23−24), 2151−2155.
(18) Yi, M.; Xie, M.; Shao, Y.; Li, W.; Ling, H.; Xie, L.; Yang, T.; Fan, Q.; Zhu, J.; Huang, W. Light Programmable/erasable Organic Field-Effect Transistor Ambipolar Memory Devices Based on the Pentacene/PVK Active Layer. *J. Mater. Chem. C* **2015**, *3* (20), 5220−5225.
(19) Guo, Y.; Di, C. a.; Ye, S.; Sun, X.; Zheng, J.; Wen, Y.; Wu, W.; Yu, G.; Liu, Y. Multibit Storage of Organic Thin-Film Field-Effect Transistors. *Adv. Mater.* **2009**, *21* (19), 1954−1959.
(20) Podzorov, V.; Gershenson, M. Photoinduced Charge Transfer Across the Interface Between Organic Molecular Crystals and Polymers. *Phys. Rev. Lett.* **2005**, *95* (1), 016602.
(21) Salleo, A.; Street, R. Light-induced Bias Stress Reversal in Polyfluorene Thin-film Transistors. *J. Appl. Phys.* **2003**, *94* (1), 471−479.
(22) Feng, C.; Mei, T.; Hu, X.; Pavel, N. A Pentacene Field-Effect Transistor with Light-Programmable Threshold Voltage. *Org. Electron.* **2010**, *11* (11), 1713−1718.
(23) Hu, Y.; Dong, G.; Liu, C.; Wang, L.; Qiu, Y. Dependency of Organic Phototransistor Properties on the Dielectric Layers. *Appl. Phys. Lett.* **2006**, *89* (7), 072108.
(24) Zhuang, J.; Lo, W. S.; Zhou, L.; Sun, Q. J.; Chan, C. F.; Zhou, Y.; Han, S. T.; Yan, Y.; Wong, W. T.; Wong, K. L.; Roy, V. A. L. Photo-Reactive Charge Trapping Memory Based on Lanthanide Complex. *Sci. Rep.* **2015**, *5*, 14998.
(25) Mei, J.; Leung, N. L.; Kwok, R. T.; Lam, J. W.; Tang, B. Z. Aggregation-Induced Emission: Together We Shine, United We Soar! *Chem. Rev.* **2015**, *115* (21), 11718−11940.
(26) Frolova, L. A.; Troshin, P. A.; Susarova, D. K.; Kulikov, A. V.; Sanina, N. A.; Aldoshin, S. M. Photoswitchable Organic Field-effect Transistors and Memory Elements Comprising an Interfacial Photochromic Layer. *Chem. Commun.* **2015**, *51* (28), 6130−6132.
(27) Jeong, Y. J.; Yoo, E. J.; Kim, L. H.; Park, S.; Jang, J.; Kim, S. H.; Lee, S. W.; Park, C. E. Light-Responsive Spiropyran Based Polymer Thin Films for Use in Organic Field-Effect Transistor Memories. *J. Mater. Chem. C* **2016**, *4* (23), 5398−5406.
(28) Wang, H.; Ji, Z.; Shang, L.; Chen, Y.; Han, M.; Liu, X.; Peng, Y.; Liu, M. Nonvolatile Nano-Crystal Floating Gate OFET Memory with Light Assisted Program. *Org. Electron.* **2011**, *12* (7), 1236−1240.
(29) Zhou, Y.; Han, S. T.; Chen, X.; Wang, F.; Tang, Y. B.; Roy, V. An Upconverted Photonic Nonvolatile Memory. *Nat. Commun.* **2014**, *5*, 4720.
(30) Saragi, T. P. I.; Pudzich, R.; Fuhrmann, T.; Salbeck, J. Organic Phototransistor Based on Intramolecular Charge Transfer in a Bifunctional Spiro Compound. *Appl. Phys. Lett.* **2004**, *84* (13), 2334−2336.
(31) Rim, Y. S.; Yang, Y. M.; Bae, S. H.; Chen, H.; Li, C.; Goorsky, M. S.; Yang, Y. Ultrahigh and Broad Spectral Photodetectivity of an Organic−inorganic Hybrid Phototransistor for Flexible Electronics. *Adv. Mater.* **2015**, *27* (43), 6885−6891.
(32) Lee, H.; Nam, S.; Kwon, H.; Lee, S.; Kim, J.; Lee, W.; Lee, C.; Jeong, J.; Kim, H.; Shin, T. J.; Kim, Y. Solution-processable All-small Molecular Bulk Heterojunction Films for Stable Organic Photodetectors: Near UV and Visible Light Sensing. *J. Mater. Chem. C* **2015**, *3* (7), 1513−1520.
(33) Zhou, L.; Han, S. T.; Shu, S.; Zhuang, J.; Yan, Y.; Sun, Q. J.; Zhou, Y.; Roy, V. A. L. Localized Surface Plasmon Resonance-Mediated Charge Trapping/Detrapping for Core−Shell Nanorod-Based Optical Memory Cells. *ACS Appl. Mater. Interfaces* **2017**, *9* (39), 34101−34110.
(34) Liu, X.; Dong, G.; Zhao, D.; Wang, Y.; Duan, L.; Wang, L.; Qiu, Y. The understanding of the memory nature and mechanism of the Ta_2O_5-gate-dielectric-based organic phototransistor memory. *Org. Electron.* **2012**, *13* (12), 2917−2923.
(35) Chen, F. C.; Chang, H. F. Photoerasable organic nonvolatile memory devices based on hafnium silicate insulators. *IEEE Electron Device Lett.* **2011**, *32* (12), 1740−1742.
(36) Chuang, C. S.; Chen, F. C.; Shieh, H. P. D. Organic thin-film transistors with reduced photosensitivity. *Org. Electron.* **2007**, *8* (6), 767−772.
(37) Shih, C. C.; Chiu, Y. C.; Lee, W. Y.; Chen, J. Y.; Chen, W. C. Conjugated Polymer Nanoparticles as Nano Floating Gate Electrets for High Performance Nonvolatile Organic Transistor Memory Devices. *Adv. Funct. Mater.* **2015**, *25* (10), 1511−1519.
(38) Baeg, K. J.; Khim, D.; Kim, D. Y.; Jung, S. W.; Koo, J. B.; Noh, Y. Y. Organic Nano-Floating-Gate Memory with Polymer:[6,6]-phenyl-C61 Butyric Acid Methyl Ester Composite Films. *Jpn. J. Appl. Phys.* **2010**, *49* (5S1), 05EB01.
(39) Zhou, Y.; Han, S. T.; Yan, Y.; Huang, L. B.; Zhou, L.; Huang, J.; Roy, V. Solution Processed Molecular Floating Gate for Flexible Flash Memories. *Sci. Rep.* **2013**, *3*, 3093.
(40) Jeong, Y. J.; Yun, D. J.; Kim, S. H.; Jang, J.; Park, C. E. Photoinduced Recovery of Organic Transistor Memories with

DOI: 10.1021/acsami.8b02560
ACS Appl. Mater. Interfaces 2018, 10, 18281−18288

Photoactive Floating-Gate Interlayers. *ACS Appl. Mater. Interfaces* **2017**, *9* (13), 11759−11769.
(41) Nam, S.; Han, H.; Seo, J.; Song, M.; Kim, H.; Anthopoulos, T. D.; McCulloch, I.; Bradley, D. D.; Kim, Y. Ambipolar Organic Phototransistors with p-Type/n-Type Conjugated Polymer Bulk Heterojunction Light-Sensing Layers. *Adv. Electronic Mater.* **2016**, *2* (12), 1600264.
(42) Han, H.; Lee, C.; Kim, H.; Seo, J.; Song, M.; Nam, S.; Kim, Y. Strong Composition Effects in All-Polymer Phototransistors with Bulk Heterojunction Layers of p-type and n-type Conjugated Polymers. *ACS Appl. Mater. Interfaces* **2017**, *9* (1), 628−635.
(43) Nam, S.; Seo, J.; Han, H.; Kim, H.; Bradley, D. D. C.; Kim, Y. Efficient Deep Red Light-Sensing All-Polymer Phototransistors with p-type/n-type Conjugated Polymer Bulk Heterojunction Layers. *ACS Appl. Mater. Interfaces* **2017**, *9* (17), 14983−14989.
(44) Lee, C.; Lee, S.; Kim, H.; Kim, Y. UV-Sensing Semitransparent Organic Field-Effect Transistors with Wide Bandgap Small Molecular Channel and Polymeric Gate-Insulating Layers. *Adv. Electronic Mater.* **2017**, *3* (10), 1700162.
(45) Yen, H. J.; Wu, J. H.; Wang, W. C.; Liou, G. S. High-Efficiency Photoluminescence Wholly Aromatic Triarylamine-based Polyimide Nanofiber with Aggregation-Induced Emission Enhancement. *Adv. Opt. Mater.* **2013**, *1* (9), 668−676.
(46) Yen, H. J.; Chen, C. J.; Liou, G. S. Novel High-efficiency PL Polyimide Nanofiber Containing Aggregation-Induced Emission (AIE)-active Cyanotriphenylamine Luminogen. *Chem. Commun.* **2013**, *49* (6), 630−632.
(47) Tang, B.; Hong, Y.; Chen, S.; Kwok, R. T. K. Water-Soluble AIE Luminogen for Monitoring and Retardation of Amyloid Fibrillation of Insulin, U.S. Patent 8,679,738 B2, March 25, 2014.
(48) Tang, B.; Lam, W. Y.; Liu, J.; Mahtab, F. Silica Nanoparticles with Aggregation Induced Emission Characteristics as Fluorescent Bioprobe for Intracellular Imaging and Protein Carrier, U.S. Patent Application US20130210047A1, 2013.
(49) Han, T.; Deng, H.; Yu, C. Y. Y.; Gui, C.; Song, Z.; Kwok, R. T.; Lam, J. W.; Tang, B. Z. Functional isocoumarin-containing polymers synthesized by rhodium-catalyzed oxidative polycoupling of aryl diacid and internal diyne. *Polym. Chem.* **2016**, *7* (14), 2501−2510.
(50) Cheng, S. H.; Hsiao, S. H.; Su, T. H.; Liou, G. S. Novel aromatic poly(amine-imide)s bearing a pendent triphenylamine group: Synthesis, thermal, photophysical, electrochemical, and electrochromic characteristics. *Macromolecules* **2005**, *38* (2), 307−316.
(51) Oishi, Y.; Ishida, M.; Kakimoto, M. A.; Imai, Y.; Kurosaki, T. Preparation and properties of novel soluble aromatic polyimides from 4,4′-diaminotriphenylamine and aromatic tetracarboxylic dianhydrides. *J. Polym. Sci., Part A: Polym. Chem.* **1992**, *30* (6), 1027−1035.
(52) Kind, H.; Yan, H.; Messer, B.; Law, M.; Yang, P. Nanowire Ultraviolet Photodetectors and Optical Switches. *Adv. Mater.* **2002**, *14* (2), 158.
(53) Zhang, X.; Jie, J.; Zhang, W.; Zhang, C.; Luo, L.; He, Z.; Zhang, X.; Zhang, W.; Lee, C.; Lee, S. Photoconductivity of a Single Small-Molecule Organic Nanowire. *Adv. Mater.* **2008**, *20* (12), 2427−2432.
(54) Kung, S. C.; van der Veer, W. E.; Yang, F.; Donavan, K. C.; Penner, R. M. 20 μs Photocurrent Response from Lithographically Patterned Nanocrystalline Cadmium Selenide Nanowires. *Nano Lett.* **2010**, *10* (4), 1481−1485.
(55) Guo, N.; Hu, W.; Liao, L.; Yip, S.; Ho, J. C.; Miao, J.; Zhang, Z.; Zou, J.; Jiang, T.; Wu, S.; Chen, X.; Lu, W. Anomalous and Highly Efficient InAs Nanowire Phototransistors Based on Majority Carrier Transport at Room Temperature. *Adv. Mater.* **2014**, *26* (48), 8203−8209.
(56) Baeg, K. J.; Binda, M.; Natali, D.; Caironi, M.; Noh, Y. Y. Organic Light Detectors: Photodiodes and Phototransistors. *Adv. Mater.* **2013**, *25* (31), 4267−4295.

DOI: 10.1021/acsami.8b02560
ACS Appl. Mater. Interfaces 2018, 10, 18281−18288